Progress In Electromagnetics Research Letters, Vol. 101, 19–27, 2021

Design of a Novel Microwave Plasma Source Based on Ridged Waveguide

Pingping Deng[1], Wei Xiao[1], Fengxia Wang[2], and Zhengping Zhang[1, *]

Abstract—The tapered waveguide as a microwave plasma excitation structure is widely used in the industrial field. However, it needs high input microwave power to ignite and sustain plasma because its electric field is not sufficiently focused in the discharge area. In order to solve this problem, this paper proposes a novel microwave plasma source based on a ridged waveguide. The structure of the proposed microwave plasma source is optimized to focus the electric field in the discharge region by electromagnetic calculations before the plasma excitation. Then, the equivalent circuit model is used to analyze the impedance matching characteristics of the novel device after the plasma excitation. In order to validate this device, a microwave plasma system is built to measure the plasma exciting power and sustaining power in both air and argon at atmospheric pressure. The simulation and experiment are carried out in both tapered waveguide and the proposed device. Simulation results show the electric field of the ridged waveguide is 1.9 times of that of the tapered waveguide when the input power is 1500 W. Moreover, in the experiments, the exciting power and sustaining power of the air and argon plasma in the novel device are lower than those of the tapered waveguide at different gas flow rates.

1. INTRODUCTION

Microwave plasma is widely used in industrial fields, such as nanomaterial synthesis, material surface treatment, and sterilization [1–4] due to the advantages of high electron and gas temperature, a wide range of working pressure, and no electrodes [5, 6]. Many researchers have obtained microwave-induced plasma by the tapered waveguide [7–9]. For example, Yang et al. used a tapered waveguide to conduct a numerical study on the continuous discharge of argon under atmospheric pressure [10]. A configuration based on a high-quality cylindrical resonator was presented by Baeva et al. [11]. Here, the microwave is coupled via a tapered rectangular waveguide to the high-quality cylindrical resonator. Kim et al. studied long-slit microwave plasma through tapered waveguides [12].

However, current tapered waveguide mainly enhances the electric field through the compression of the narrow side of the waveguide [9, 13, 14]. The inadequate electric field focusing of the structure results in higher energy consumption. Specifically, the plasma's exciting power and sustaining power are relatively high [10, 15]. Recently, improved models of tapered waveguides have been reported. For example, Zhang et al. proposed a dual-port tapered waveguide structure [16]. A line-shaped microwave plasma source was proposed by Abdel-Fattah et al. [17]. Moisan et al. presented a waveguide-based launcher (surfaguide) that can efficiently generate and sustain long plasma columns [18]. However, in these structures, the insufficient electric field focusing and high energy consumption of the tapered waveguide are still not fully solved. Therefore, this paper proposes a novel microwave plasma source (MPS) based on a ridged waveguide to solve this problem. In tapered waveguide and ridged waveguide, the electric field is mainly focused in the discharge area and reaches the maximum value there. In the

Received 25 August 2021, Accepted 22 October 2021, Scheduled 29 October 2021

* Corresponding author: Zhengping Zhang (zpzhang@gzu.edu.cn).

[1] College of Big Data and Information Engineering, Guizhou University, Guiyang 550025, China. [2] State Key Laboratory of Efficient Utilization for Low Grade Phosphate Rock and Its Associated Resources, Wengfu Group, Guiyang 550014, China.

simulation, the maximum electric field values of the tapered waveguide and the ridged waveguide are respectively 6.76×10^4 V/m and 1.33×10^5 V/m when the input power is 1500 W. In the experiment, the energy consumption of the devices is analyzed emphatically. The main method of our analysis is to compare the exciting power and sustaining power of the plasma of these two devices. Air and argon are used as working gases. Under atmospheric pressure, these two parameters can be measured at different gas flow rates [19, 20]. Lower power value (exciting power; sustaining power) shows lower energy consumption required by the plasma source. It is worth noting that the experimental results show that compared with the traditional tapered waveguide, the plasma exciting power and sustaining power of the ridged waveguide are lowered by 27.5% and 30%, respectively. This is consistent with that the maximum electric field value of the ridged waveguide is 1.9 times of that of the tapered waveguide in the electric field simulation. Therefore, the required energy consumption for plasma exciting and sustaining of the ridged waveguide is lower. To the best of the authors' knowledge, this structure has never been used as an MPS.

2. OPTIMIZATION OF THE DEVICE

2.1. Structure Description

To maximize the electric field intensity of the discharge area, the dimensions of the ridged waveguide have been optimized to the best value. The specifications are shown in Table 1. Due to a large number of parameters, this paper only focuses on the three parameters that have a great impact on the electric field intensity. They are the wide side (G), the half-length of the narrow side (H) of the resonant cavity, and the height of the metal ridge (N). As shown in Figs. 1(a), (b), and (c), we can conclude that the electric field intensity varies with the sizes of the device and reaches a maximum value at a certain position. Therefore, this size is optimal. The optimal dimensions of the wide side (G), the half length of the narrow side (H) of the resonant cavity, and the height (N) of the metal ridge are 87 mm, 42.5 mm, and 10 mm, respectively. Fig. 2 is a cross-sectional view of the waveguide of the final structure. It is based on the standard rectangular waveguide BJ22, which is short-circuited at the end. The operating frequency of incident microwaves is 2.45 GHz. The total length of the structure is designed to be 156 mm. In the discharge area, a quartz tube with an inner diameter of 26 mm and an outer diameter of 28 mm passes through the center of the wide wall of the waveguide.

Table 1. Explanation of each size of the proposed microwave plasma source.

Symbol Name	Physical Meaning	Length (mm)
A	Height of the transition section	54
B	Half Width of the transition section	50
α	Slant angle of the transition section	27°
F	Length of the ridge	29
G	Length of the cavity	87
R_1	Outer diameter of the quartz tube	28
R_2	Inner diameter of the quartz tube	26
H	half width of the cavity	42.55
I	Height of the cavity	34
M	Width of the ridge	50
N	Height of the ridged	10
O	Height of the impedance matching segment	34
V	Width of the impedance matching segment	68.4

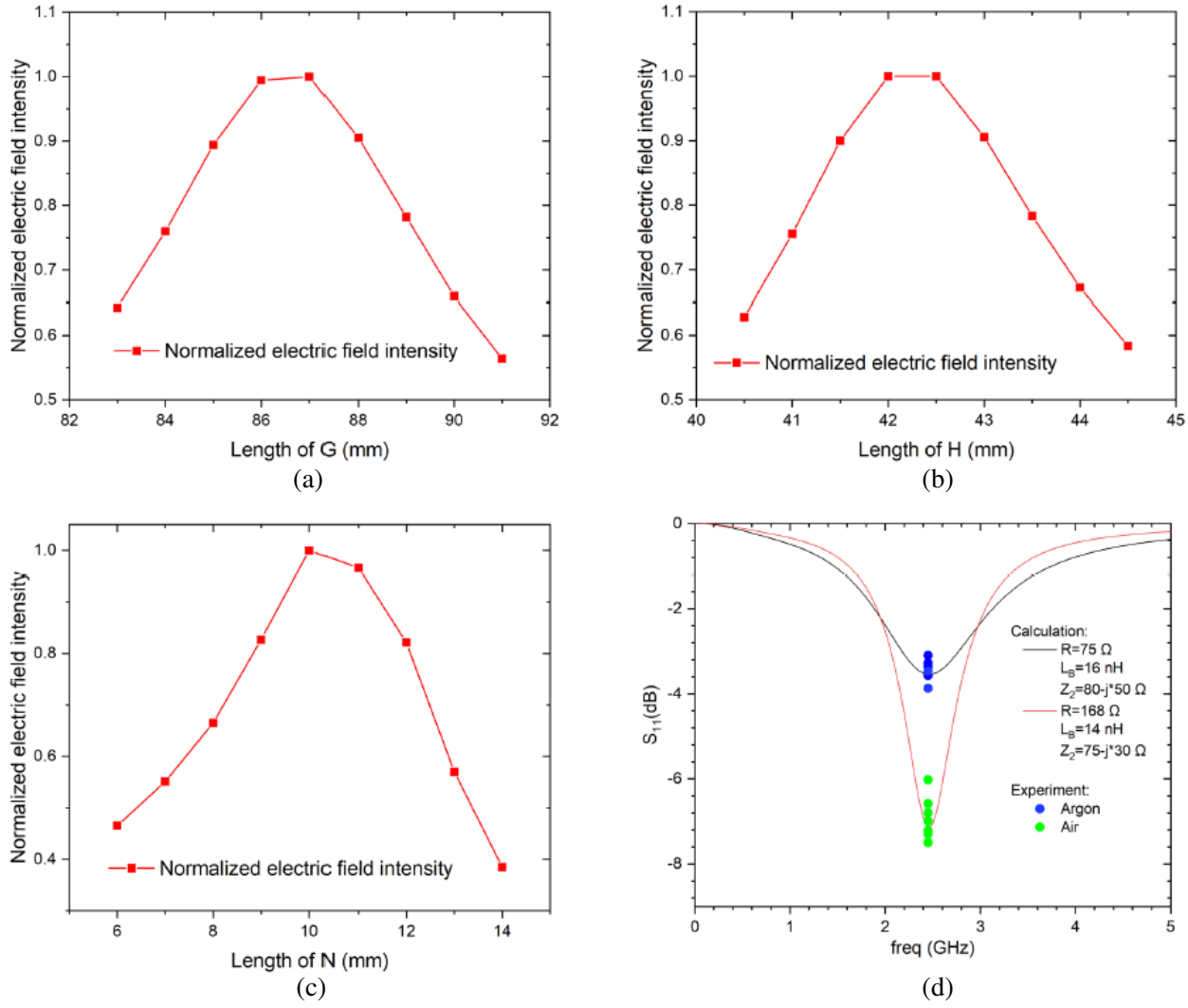

Figure 1. The maximum electric field intensity changes with the dimensions of the ridged waveguide: (a) Length of G, (b) length of H, (c) length of N; (d) fitting the experimentally described electrodynamic characteristics to the analytical ones [18].

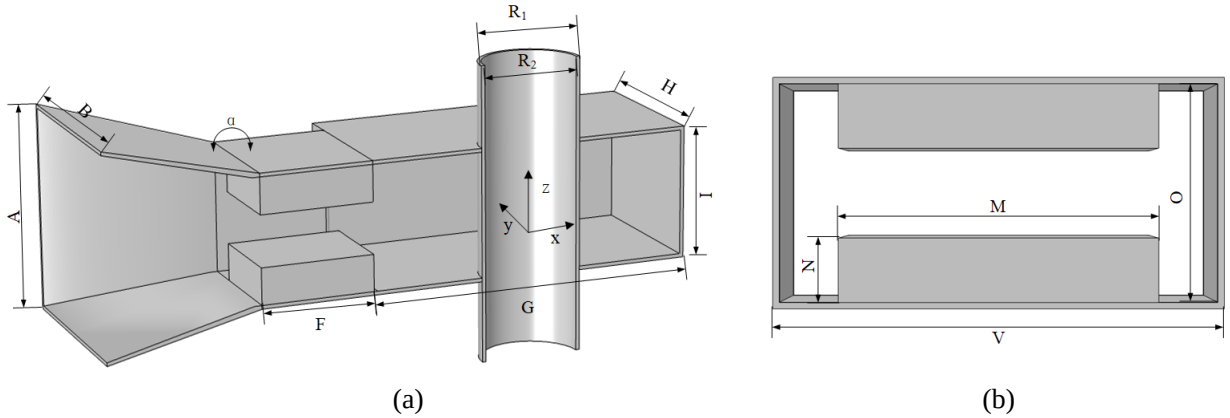

Figure 2. Cross-sectional view of the ridged waveguide. (a) X-Z cross section, (b) Y-Z section.

2.2. Simulation Method before Plasma Excitation

Before experiments, a three-dimensional (3D) electromagnetic model is built by the commercial software COMSOL Multiphysics. In our calculations, a mesh with 280 644 elements has been used. The simulated model is optimized to the best dimensions to maximize the electric field in the discharge area of the device. The microwave field of the discharge tube is observed intuitively and compared exactly with each other. Fig. 4(b) shows the optimized electric field distribution of the device before plasma excitation. The Helmholtz equation is used to describe the electric field E,

$$\nabla \times \left(\mu_r^{-1} \nabla \times E\right) - k_0^2 \left(\varepsilon_r - \frac{j\sigma}{\omega \varepsilon_0}\right) E = 0 \tag{1}$$

where μ_r is the relative permeability (usually equals 1), k_0 the free-space wave number, ε_r the real part of the permittivity of the medium, and its value is 4.2; σ represents the conductivity, and its value is 0; ε_0 is the permittivity of vacuum, and ω is the incident electromagnetic wave's angular frequency.

2.3. Equivalent Circuit Model after Plasma Excitation

After this structure was optimized by three-dimensional electromagnetic simulation, the electric field in the discharge area reached its maximum value. In order to analyze the impedance matching of the proposed device after plasma excitation, an equivalent circuit model is adopted, which is shown in Fig. 3. The equivalent circuit of the microwave plasma source contains a two-port network. In this equivalent circuit, the part of the ridged waveguide transmission line is equivalent to the parallel connection of impedance Z_1, inductance L_A, and capacitance C. The plasma current effect is equivalent to the series connection of inductance L_B and impedance Z_2, and then parallel to resistance R. In this way, an equivalent circuit of a microwave plasma source containing plasma is formed, as shown in Fig. 3. It is calculated using the Advanced Design System (ADS) simulation tool and using the ABCD-matrix & S-parameter convergence [21].

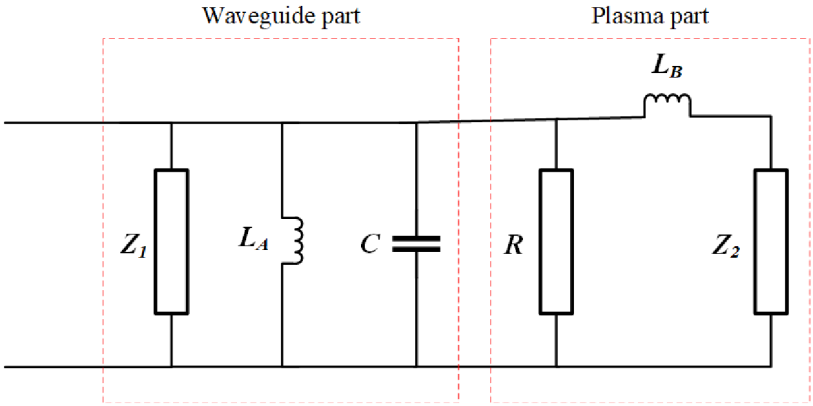

Figure 3. Diagram of the equivalent electrical circuit of the MPS.

3. RESULT AND DISCUSSION

3.1. Simulation Results

As shown in Fig. 4(a), in the electric field simulation part, the electric field distribution of the tapered waveguide was also simulated. The same calculations were performed for the tapered waveguide and ridged waveguide. When the port excitation is 1500 W and the operating frequency is 2.45 GHz, the maximum electric field intensities of the tapered waveguide and ridged waveguide are 6.76×10^4 V/m and 1.33×10^5 V/m, respectively (Fig. 4). We can conclude that the electric field intensity of the second

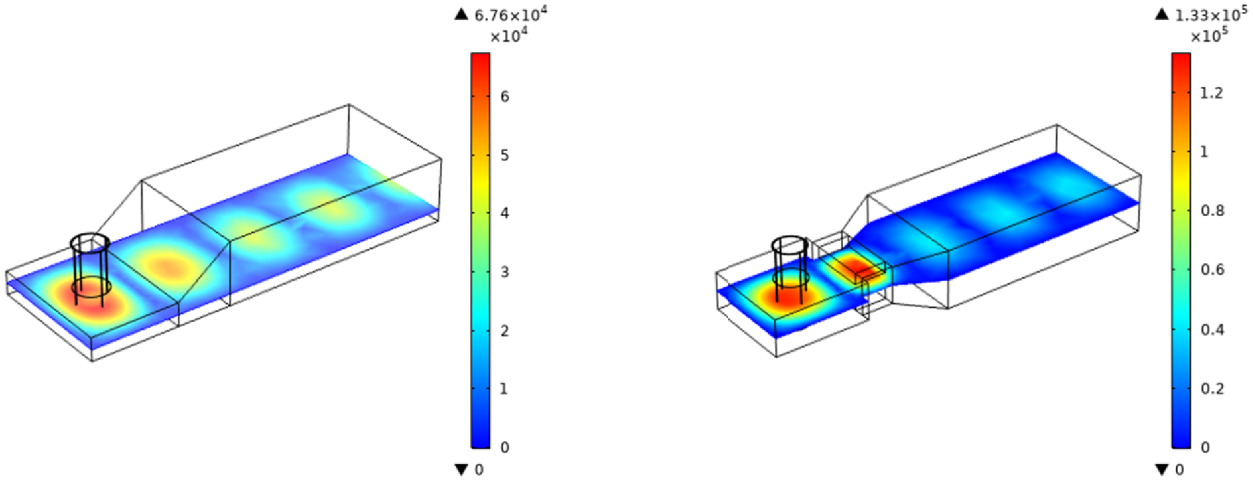

Figure 4. Distributions of the electric field intensity (V/m) in two apparatuses: (a) the tapered waveguide, (b) the ridged waveguide.

waveguide is 1.9 times of that of the first waveguide. Therefore, the performance of the ridged waveguide is better than that of the tapered waveguide in the 3D electromagnetic simulation.

As shown in Fig. 4(b), when the working gas is introduced, the high electric field intensity of the ridged waveguide in the discharge area will excite the gas into plasma. The plasma impedance is a key issue of the atmospheric pressure microwave plasma source, and the plasma impedance is the main factor that controls the power transmission from the microwave generator to the plasma source. Therefore, it is important to study the plasma impedance in an atmospheric pressure plasma source excited by microwaves. In [22], by simulating the electromagnetic field distribution of the ridged waveguide plasma source, using the method described in [23–25], it was determined that $Z_1 = 56 + j * 124\,\Omega$, $L_A = 4\,\text{nH}$, $C = 2\,\text{pF}$. During the experiment, we found that the plasma impedance was related to the gas composition and flow rate of the gas. After the gas composition is determined, different gas flow rates correspond to different plasma impedances [26], and the corresponding scattering-parameter (S_{11}) is also different, which describes the electrodynamic characteristics of the MPS. Therefore, the unknown elements R, L_B, and Z_2 could be determined by fitting the experimentally described electrodynamic characteristics to the analytical ones. An example of such a fitting is presented in Fig. 1(d). It can be seen from Fig. 1(d) that the scattering-parameter (S_{11}) values [27] of air and argon at different flow rates can fit well with the characteristic curve corresponding to the specific value of R, L_B, Z_2. For resistance $R = 75\,\Omega$, inductance $L_B = 2\,\text{nH}$, and impedance $Z_2 = 80 - j * 50\,\Omega$ satisfied the good fitting in the entire range of the argon flow rate. At the same time, Fig. 1(d) also shows that when the resistance $R = 168\,\Omega$, the inductance $L_B = 14\,\text{nH}$, and the impedance $Z_2 = 75 - j * 30\,\Omega$. It also achieved good fitting in the entire range of the air flow rate. They correspond to the plasma part of the circuit of other microwave plasmas [28, 29].

3.2. Experiment Results

Figure 5 shows photographs of the manufactured product. The microwave plasma source consists of a 2.45 GHz microwave generator of maximum power 3000 W and a TE_{10} model rectangular waveguide connected to a customized ridged waveguide using a BJ22 waveguide. The reflected power is deflected by the ferrite circulator to the water load connected to the third port of the circulator. The bidirectional coupler and AV2433 microwave power meter are used to couple and measure the incident and reflected power, respectively. As gas flow meters, KT-C4Z Intelligent Gas Supply System and DK800-6 Glass Rotameter can respectively provide air and argon at different flow rates. Two hollow hoses that conduct air in opposite directions are used to sustain the vortex. Generally, this vortex helps stabilize the plasma

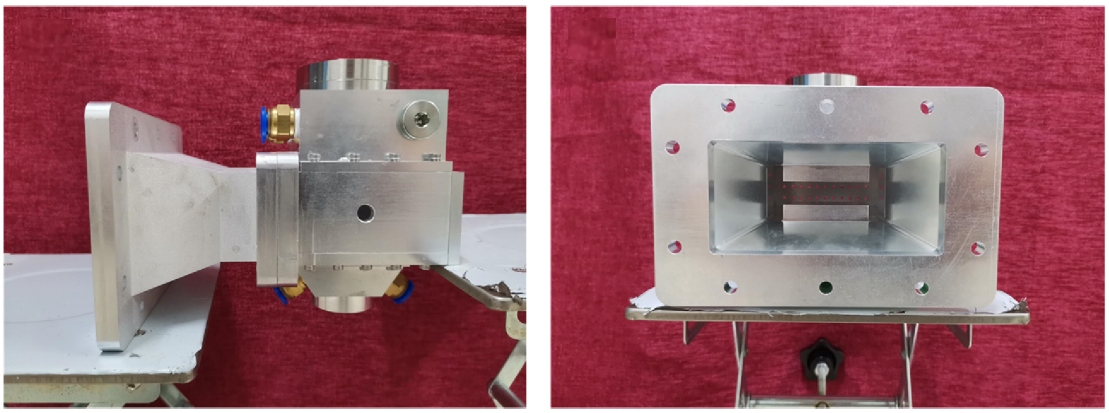

(a) (b)

Figure 5. Photograph of the ridged waveguide: (a) side view, (b) cross-sectional view.

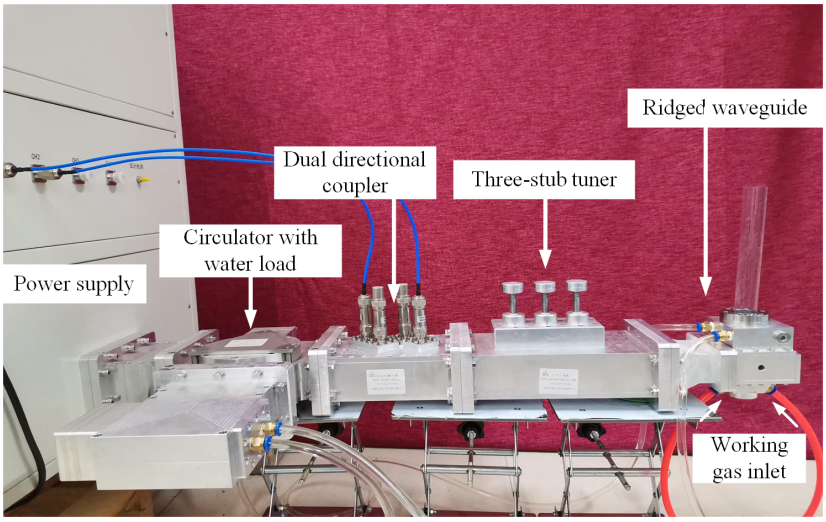

Figure 6. Photograph of the experimental set-up.

torch, especially at high gas flow rates [30]. In addition, it can also protect the quartz tube from thermal damage caused by the high temperature of the plasma.

In the experiment, air plasma and argon plasma's minimum exciting power and sustaining power can be obtained at different gas flow rates. Before the experiment, we prepared a sharp-ended copper wire to provide seed electrons in the discharge area to ignite the plasma. A schematic drawing of the experimental setup is shown in Fig. 6.

3.2.1. Exciting Power

The exciting power is measured here. We introduced $180L/h$ of air, and the incident power of 500 W was gradually increased at intervals of 50 W. As the power value increases, the air in the discharge tube will be excited into plasma at a certain power value. The power value at this moment is recorded as the minimum exciting power. Repeat the measurement at all flow rates of 180, 300, 540, 600, 900, 1080, 1200, $1500L/h$. Because the flow meters of argon is DK800-6 Glass Rotameter, for the convenience of choosing the value, the flow rate of argon is respectively taken as 180, 500, 800, 1000, 1200, 1500,

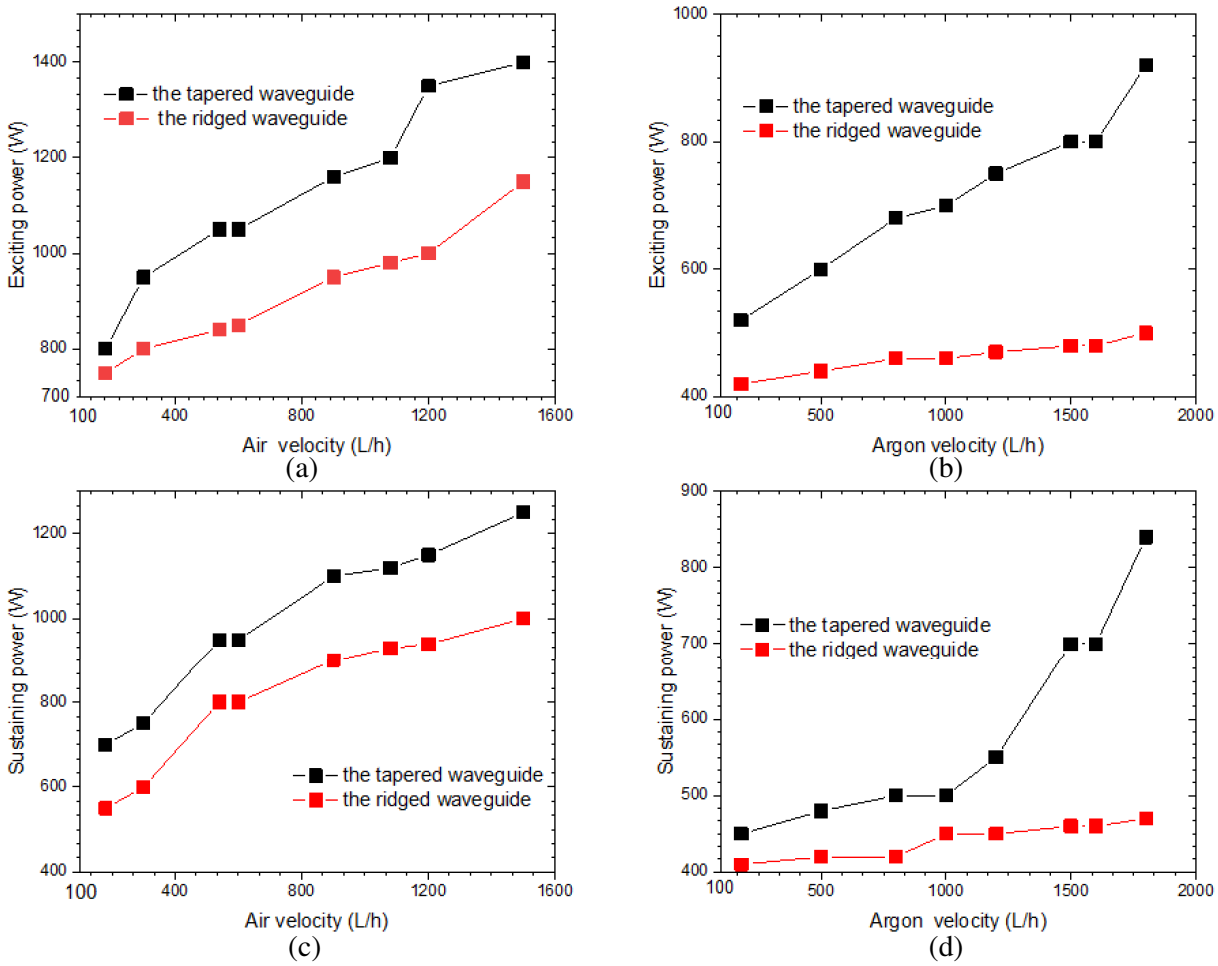

Figure 7. (a), (b) Variation of exciting power with flow rate of air and argon respectively; (c), (d) variation of sustaining power with flow rate of air and argon, respectively.

1600, $1800L/h$. Equal measurement operations have been done for the argon. The results are shown in Figs. 7(a), (b). We can see that as the gas flow rate increases, the plasma's exciting power also increases. It is worth noting that whether air or argon is used as the working gas, the power value in the ridged waveguide is significantly lower than that in the tapered waveguide. The former is about 27% lower than the latter. There are potential applications in some gas processing industries because ridged waveguides consume less energy at the same flow rate.

3.2.2. Sustaining Power

In our further work, after the plasma was excited, we measured the plasma sustaining power of air and argon at different flow rates. After the plasma is excited at a certain flow rate, the power is gradually reduced. The accompanying phenomenon is that the plasma torch becomes smaller and smaller until it goes out. The power value at the previous moment is recorded as the minimum sustaining power. As shown in Figs. 7(c), (d), as the gas flow rate increases, the increasing trend of the sustaining power is the same as the excitation power. Moreover, we can still see that whether air or argon is used as the working gas, the sustaining power value of the ridged waveguide is significantly lower than that of the tapered waveguide. The first waveguide is 30% lower than the second waveguide. This is very consistent with our previous simulation results.

4. CONCLUSION

In this paper, we propose a novel type of microwave plasma source based on ridged waveguide. Three-dimensional electromagnetic simulations show that the maximum electric field intensity of the ridged waveguide is 1.9 times of that of the tapered waveguide. The electric field of the ridged waveguide is more fully concentrated in the discharge area than the tapered waveguide. Two experiments were performed to measure the minimum excitation power and sustaining power of the plasma. One result shows that the gas in the proposed device can be excited into plasma at relatively low power compared with the traditional tapered waveguide. The plasma excitation power of the ridged waveguide is 27.5% lower than that of the tapered waveguide. Another result shows that after plasma excitation, the plasma sustaining power of the novel device is significantly lower than that of the traditional tapered waveguide at the same gas flow rate. The plasma sustaining power of the former is 30% lower than that of the latter. This is consistent with the simulation results of the three-dimensional electromagnetic field. The required energy consumption for plasma exciting and sustaining of the ridged waveguide is lower. This means that in exhaust gas treatment, the plasma generated in the proposed device can treat a larger amount of exhaust gas per unit of power. Therefore, it has a broader application prospect.

ACKNOWLEDGMENT

This work is supported in part by the National Natural Science Foundation of China under Grant 62101146, in part by Guizhou Provincial Science and Technology Projects under grant No. ZK2021-general 298 and in part by the State Key Laboratory of Efficient Utilization for Low Grade Phosphate Rock and Its Associated Resources under grant No. WFKF2020-09.

REFERENCES

1. Jaeho, K., O. Hiroyuki, and K. Makoto, "Control of plasma-dielectric boundary sheath potential for the synthesis of carbon nanomaterials in surface wave plasma CVD," *IEEE Transactions on Plasma Science*, Vol. 43, No. 1, 480–484, 2015.
2. Moon, S. Y., J. W. Han, and W. Choe, "Feasibility study of material surface treatment using an atmospheric large-area glow plasma," *J. Thin Solid Films*, Vol. 506, 355–359, May 2006.
3. Laroussi, M., "Sterilization of contaminated matter with an atmospheric pressure plasma," *IEEE Transactions on Plasma Science*, Vol. 24, No. 3, 1188–1191, 2002.
4. Hiro, K., *Plasma Electronic Engineering*, OHM & Science Press, Beijing, China, 2002.
5. Moon, S. Y., W. Choe, H. S. Uhm, et al., "Characteristics of an atmospheric microwave-induced plasma generated in ambient air by an argon discharge excited in an open-ended dielectric discharge tube," *J. Physics of Plasmas*, Vol. 9, No. 9, 4045–4051, 2002.
6. Zhao, Q., S. Z. Liu, and H. H. Tong, *Plasma Technology and Its Applications*, National Defence Industry Press, Beijing, 2009.
7. Zheng, Z., Z. Chen, P. Liu, et al., "Study on Argon plasma jets at atmospheric pressure in ambient air excited by surface waves," *IEEE Transactions on Plasma Science*, Vol. 24, No. 4, 911–916, 2014.
8. Levko, D., A. Sharma, and L. L. Raja, "Plasmas generated in bubbles immersed in liquids: Direct current streamers versus microwave plasma," *Journal of Physics D: Applied Physics*, Vol. 49, No. 28, 285205, 2016.
9. Chapman, A., W. Luo, et al., "Plasma generation by dielectric resonator arrays," *Plasma Sources Science & Technology*, 2016.
10. Yang, Y., W. Hua, and S. Y. Guo, "Numerical study on microwave-sustained argon discharge under atmospheric pressure," *Physics of Plasmas*, Vol. 21 No. 4, 7–963, 2014.
11. Baeva, M., et al., "Pulsed microwave discharge at atmospheric pressure for NOx decomposition," *Plasma Sources Science & Technology*, 2002.

12. Kim, H. J., J. J. Choi, and J. M. Hong, "Uniform long-slit microwave plasma generation from a longitudinal-section electric mode coupling," *IEEE Transactions on Plasma Science*, Vol. 34, No. 4, 1576–1578, 2006.
13. Kabouzi, Y., D. B. Graves, E. Castaños-Martínez, and M. Moisan, "Modeling of atmospheric-pressure plasma columns sustained by surface waves," *Phys. Rev. E*, Vol. 75, 016402, 2007.
14. Chaichumporn, C., P. Ngamsirijit, N. Boonklin, et al., "Design and construction of 2.45 GHz microwave plasma source at atmospheric pressure," *Procedia Engineering*, Vol. 8, 94–100, 2011.
15. Kuo, S. P., D. Bivolaru, H. Lai, et al., "Characteristics of an arc-seeded microwave plasma torch," *IEEE Transactions on Plasma Science*, Vol. 32, No. 4, 1734–1741, 2015.
16. Zhang, D., R. Zhou, X. Q. Yang, et al., "Design of novel dual-port tapered waveguide plasma apparatus by numerical analysis," *Physics of Plasmas*, Vol. 23, No. 7, 2016.
17. Abdel-Fattah, E., H. Shindo, R. Sabry, and A. El Kotp, "Experimental and numerical investigations of line-shaped microwave argon plasma source," *Progress In Electromagnetics Research M*, Vol. 43, 183–192, 2015.
18. Moisan, M., Z. Zakrzewski, R. Pantel, et al., "A waveguide-based launcher to sustain long plasma columns through the propagation of an electromagnetic surface wave," *IEEE Transactions on Plasma Science*, Vol. 12, No. 3, 203–214, 1984.
19. Iio, S., K. Yanagisawa, C. Uchiyama, et al., "Influence of gas flow on argon microwave plasma jet at atmospheric pressure," *Surface & Coatings Technology*, Vol. 206, No. 6, 1449–1453, 2011.
20. Zhang, W., L. Wu, J. Tao, et al., "Numerical investigation of the gas flow effects on surface wave propagation and discharge properties in a microwave plasma torch," *IEEE Transactions on Plasma Science*, Vol. 47, No. 1, 271–277, 2019.
21. Pozar, A. D. M., *Microwave Engineering*, Publishing House of Electronics Industry, Beijing, 2019.
22. Fleisch, T., Y. Kabouzi, M. Moisan, et al., "Designing an efficient microwave-plasma source, independent of operating conditions, at atmospheric pressure," *Plasma Sources Science & Technology*, Vol. 16, No. 1, 173, 2006.
23. Miotk, R. and M. Jasiński, "Investigation of the electrodynamic characteristics of 2.45 GHz microwave plasma sheet source," *IEEE MTT-S International Conference on Numerical Electromagnetic and Multiphysics Modeling and Optimization (NEMO)*, 1–4, 2019.
24. Miotk, R., M. Jasiński, and J. Mizeraczyk, "Improvement of energy transfer in a cavity-type 915-MHz microwave plasma source," *IEEE Transactions on Microwave Theory and Techniques*, Vol. 66, No. 2, 711–716, 2018.
25. Kim, J. D., H. K. Sang, H. J. Kim, et al., "Impedance measurement system for a microwave-induced plasma," *Journal of the Korean Physical Society*, Vol. 60, No. 6, 907–911, 2012.
26. Mitsugi, F., T. Ohshima, H. Kawasaki, et al., "Gas flow dependence on dynamic behavior of serpentine plasma in gliding arc discharge system," *IEEE Transactions on Plasma Science*, Vol. 42, No. 12, 3681–3686, 2014.
27. Gurel, C. S. and E. Öncü, "Interaction of electromagnetic wave and plasma slab with partially linear and sinu-soidal electron density profile," *Progress In Electromagnetics Research Letters*, Vol. 12, 171–181, 2009.
28. Miotk, R., M. Jasiński, and J. Mizeraczyk, "Equivalent circuit of a coaxial-line-based nozzleless microwave 915 MHz plasma source," *IOP Conference*, 113, 2016.
29. Miotk, R., "Equivalent circuit of a microwave plasma source for hydrogen production from liquid substances," *Przeglad Elektrotechniczny*, Vol. 1, No. 8, 31–34, 2016.
30. Nowakowska, H., M. Jasiński, and J. Mizeraczyk, "Modelling of discharge in a high-flow microwave plasma source (MPS)," *European Physical Journal D*, Vol. 67, No. 7, 1–8, 2013.